JULY 12–16
2020 VIRTUAL
JOINT AAPM | COMP MEETING
EASTERN TIME [GMT-4]

Association of lung CT voxel-based radiomics feature map with lung ventilation imaging

Z. Yang[1,2], K. Lafata[3], X. Chen[1,2], Y. Chang[1,3], F. F. Yin[1,2,3]

1 Medical Physics Graduate Program, Duke University, Durham, United States of America

2 Medical Physics Graduate Program, Duke Kunshan University, Kunshan, People's Republic of China

3 Department of Radiation Oncology, Duke University Medical Center, Durham, United States of America

DukeHealth

INTRODUCTION

The paradigm shift towards Quantitative Image Analysis (QIA) is becoming increasingly attractive for the modern imaging system. The emerging field radiomics is a typical example of QIA. Motivated by the concept that biomedical images contain pathophysiology information, the goal of radiomics is to convert the medical images into mineable high-dimensional image features, which may decipher the underlying bio-information [1]. Typical radiomics is designed to construct the feature vector from a segmented image (e.g., tumor) and analyze the results in a patent-by-patient manner. It is reasonable to the hypothesis that generalizing the conventional radiomics down to the voxel-level, i.e., voxel-based radiomics (VBR) analysis, could significantly expand the richness of the potential bio-information database and interpret the image resources more efficient.

This work investigated the association between regional pulmonary function and VBR features maps extracted from the lung computed tomography (CT) images. It is well-known that lung function can be interpreted by the expert based on CT image characteristics (e.g., bronchial thickening, honeycombing) [2]. However, such a phenomenon is typically difficult to measure and quantify. The quantitative VBR approach has the potential to reflect these observations objectively and may serve as a clinical complement to the radiologist ultimately.

PURPOSE

We employed the VBR analysis technique to investigate the potential association of spatially-encoded radiomics features extracted from lung CT images with the pulmonary function measured by ventilation scintigraphy.

METHOD

- An in-house VBR calculation platform was developed to generalize the conventional image-based radiomics to the voxel level. As in Figure 1, to extract the radiomics features at each voxel, we utilized a 3D sliding window to define a spatial kernel by aligning the voxel of interest with the centre of the window. 57 radiomics features were subsequently calculated within such a rotationally-invariant kernel. By traversing the window over the entire volume, each voxel in the original image can be expressed as a 57-dimensional radiomics feature vector. Consequently, 57 feature maps with the same spatial dimensions as the input image were generated.
- The VBR technique were employed to extracted the feature maps from total of 46 lung CT images in VAMPIRE Galligas PET and DTPA-SPECT Dataset [3]. To test the technique as a potential pulmonary biomarker, we subsequently compared the generated feature maps to corresponding reference ventilation images (RefVIs, e.g., Galligas PET or DTPA-SPECT) as ground truth for pulmonary function based on voxel-wise Spearman coefficients (ρ).
- Computed Tomography Ventilation Imaging (CTVI) is another imaging analysis technique that derives regional lung function information from respiratory-correlated CT datasets. In the VAMPIRE Challenge, total of 37 individual CTVI algorithms are submitted by participants and have been evaluated against the corresponding RefVI using Spearman coefficient [3]. Due to similar purposes, same dataset, and the same correlation analysis methods, our results can be directly compared with VAMPIRE CTVI algorithms to assess the overall performance relative to conventional 4DCT-based techniques.

Intensity-based features	1	Energy	Grey-level run-length matrix-based features	26	Short Run Emphasis
	2	Entropy		27	Long Run Emphasis
	3	Kurtosis		28	Grey Level Non-Uniformity
	4	Skewness		29	Grey Level Non-Uniformity Normalized
Grey-level co-occurrence matrix-based features	5	Auto Correlation		30	Run Length Non-Uniformity
	6	Cluster Prominence		31	Run Length Non-Uniformity Normalized
	7	Cluster Shade		32	Run Percentage
	8	Cluster Tendency		33	Low Grey Level Run Emphasis
	9	Contrast		34	High Grey Level Run Emphasis
	10	Correlation		35	Short Run Low Grey Level Emphasis
	11	Difference Entropy		36	Short Run High Grey Level Emphasis
	12	Dissimilarity		37	Long Run Low Grey Level Emphasis
	13	Energy		38	Long Run High Grey Level Emphasis
	14	Entropy		39	Grey Level Variance
	15	Homogeneity 1		40	Run Length Variance
	16	Homogeneity 2		41	Run Entropy
	17	Info Measure Correlation 1	Grey-level size zone matrix-based features	42	Small Zone Emphasis
	18	Info Measure Correlation 2		43	Large Zone Emphasis
	19	Inverse Difference Moment Normalized		44	Grey Level Non-Uniformity
	20	Inverse Difference Normalized		45	Grey Level Non-Uniformity Normalized
	21	Inverse Variance		46	Size Zone Non-Uniformity
	22	Maximum Probability		47	Size Zone Non-Uniformity Normalized
	23	Sum Average		48	Zone Percentage
	24	Sum Entropy		49	Low Grey Level Zone Emphasis
	25	Sum Variance		50	High Grey Level Zone Emphasis
				51	Small Size Low Grey Level Emphasis
				52	Small Size High Grey Level Emphasis
				53	Large Size Low Grey Level Emphasis
				54	Large Size High Grey Level Emphasis
				55	Gray Level Variance
				56	Zone Size Variance
				57	Zone Size Entropy

Table 1. All defined 57 radiomics features in our in-house developed voxel-based radiomics calculation platform.

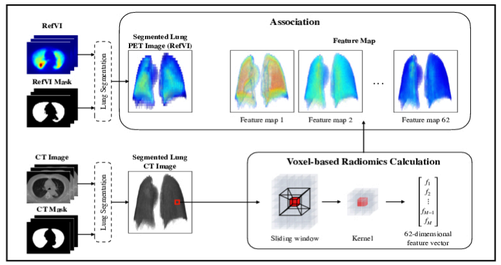

Figure 1. The overall workflow of pulmonary voxel-based radiomics feature map extraction.

RESULTS

- Figure 2 demonstrates the visual assessment of 57 feature maps extracted from one of 46 patients in VAMPIRE Dataset. The upper left panels are the original input CT and corresponding DTPA-SPECT slice. The RefVI scan exhibits defects in both the left upper lobe (LUL) and right upper lobe (RUL). A small number of feature maps successfully detect the defects in both lobes, such as feature #1, 5, 23, 34, 36, 38, 39, 50, and 52. And several other features are only able to detect the major defect that existed in the LUL, which include #10, 14, 18, 26, 30, 31, and 32. Moreover, a few features display high values in the upper lung defect region, see feature #13, 22, 27, 28, 29, 33, 35, 37, 43, 49, 51, and 53, which can be considered as negatively associated with the lung ventilation distribution.
- The box plots in figure 3 show the distributions of voxel-wise Spearman ρ evaluated between all 57 features and their corresponding RefVI scans (Galligas PET or DTPA-SPECT) for 46 patients. In each box, the central mark indicates the median, and the bottom and top edges indicate the 25th and 75th percentiles, respectively. The whiskers extend to the most extreme data points that not considered as outliers, and the outliers are plotted individually using the "+" symbol. The feature maps are ranked in descending order from left to right based on the median value of ρ.
- Considering the correlation performance for both Galligas PET and DTPA-SPECT studies, the overall highest correlations archived by feature #30, i.e., *GLRLM-based run length non-uniformity*, with $0.21 < \rho < 0.65$ (median = 0.45) for Galligas PET study and $0.29 < \rho < 0.63$ (median = 0.45) for DTPA-SPECT study. The second-highest ranked feature is #1, *I-based Energy*, with $0.05 < \rho < 0.70$ (median = 0.48) for Galligas PET study and $0.13 < \rho < 0.74$ (median = 0.43) for DTPA-SPECT study. Moreover, for both studies, the strongest negative correlations come from feature #33, 35, 37, and 51. Specifically, ρ is approximately in the range [-0.01, -0.70] (median ≈ 0.48$) and [0.09, -0.60] (median ≈ 0.30) for Galligas PET study and DTPA-SPECT study, respectively.
- Compared with 37 CTVI algorithms submitted by VAMPIRE Challenge participants [3], the correlation performance of our feature map #1 and #30 exceeds 36 algorithms, and only slightly inferior to No. 20 CTVI algorithm (range: 0.27-0.73, median: 0.49).

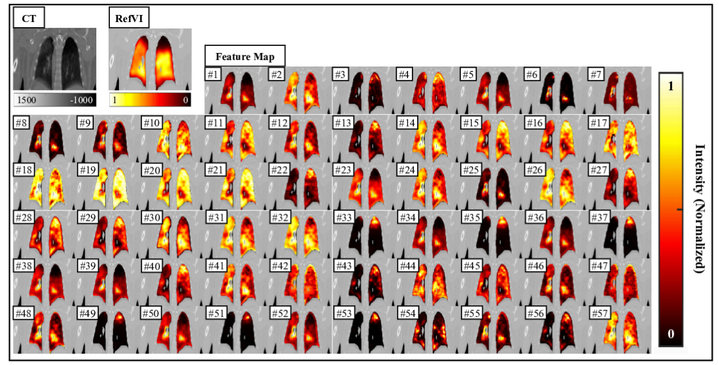

Figure 2. Visual comparison of RefVI scans (DTPA-SPECT) and corresponding 57 feature maps generated by voxel-based radiomics technique. The upper left panels are the original input time-averaged CT and corresponding DTPA-SPECT slice. The rest panels are 57 feature maps with feature # indicated in the top left corner. The RefVI is normalized to [0, 1] and superimposed over the CT at a common coronal slice location for better visualization. Similarly, each feature map is normalized with the same strategy as the RefVI to provide a similar visual contrast.

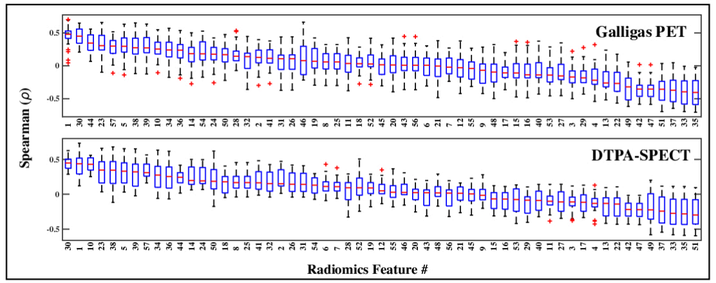

Figure 3. Spearman correlation (ρ) distributions evaluated between each voxel-based radiomics feature maps and the corresponding RefVI. Each box plot represents a specific feature maps # and RefVI modality (Galligas PET or DTPA-SPECT). In each box, the central mark indicates the median, and the bottom and top edges indicate the 25th and 75th percentiles, respectively. The whiskers extend to the most extreme data points not considered outliers, and the outliers are plotted individually using the "+" symbol. The feature maps are ranked in descending order from left to right based on the median value of ρ.

DISCUSSION AND CONCLUSIONS

- Quantitative correlation analysis identified that voxel-based radiomics feature maps extracted from lung CT images are partially associated with pulmonary function measured by Galligas PET or DTPA-SPECT ventilation image.
- *I-based energy* measures the square of intensity within the image. Higher energy corresponds to denser content. *GLRLM-based run length non-uniformity* assesses the distribution of runs over the run lengths, and a lower value indicates more homogeneity among run lengths in the image. The negatively correlated features #33, 35, 37, and 51 emphasis the low density, heterogeneous coarse structural texture. Collectively, these features together evidence that the homogeneous dense pulmonary CT image often presented as high radiotracer signal, while the regional lung CT content with low density heterogeneous coarse structural texture is often shown as a lack of radiotracer. This results are consistent with the findings based on conventional lung-segmented image-based radiomics analysis by Lafata *et al.* [2]
- Compared with the 4DCT-based CTVI method, the VBR analysis severs as several advantages: (1) the performance of its correlation distribution is better than most VAMPIRE CTVI algorithms; (2) it is easy to implement since the calculations are based on the ready-made and well-defined radiomics features; (3) it only utilizes the time-averaged CT frame instead of 4DCT, which avoids the uncertainty introduced in the deformable image registration (DIR) process.
- This study is just an application of a VBR in lung texture analysis, which is only one aspect of a typical radiomics scope. Besides that, it is reasonable to hypnosis that the VBR technique can be extended to a broader range of applications, such as differentiating benign and cancerous tissue of other body sites, characterizing intratumoral information, assisting prognostic assessment, and combining with the radiogenomic to personalize treatment, etc.

REFERENCES

[1] Gillies, Robert J., Paul E. Kinahan, and Hedvig Hricak. "Radiomics: images are more than pictures, they are data." *Radiology* 278.2 (2016): 563-577.

[2] Lafata, Kyle J., et al. "An exploratory Radiomics Approach to Quantifying pulmonary function in ct images." *Scientific reports* 9.1 (2019): 1-9.

[3] Kipritidis, John, et al. "The VAMPIRE challenge: A multi-institutional validation study of CT ventilation imaging." Medical physics 46.3 (2019): 1198-1217.

ACKNOWLEDGEMENT

Thanks to Professor John Kipritidis, Professor Henry C. Woodruff, and Professor Paul J. Keall for the generous contribution to sharing the VAMPIRE Dataset.

CONTACT INFORMATION

Poster Design and Presenter: Zhenyu Yang (zhenyu.yang893@duke.edu)

Advisor: Fang-Fang Yin (fangfang.yin@duke.edu)